JACS
JOURNAL OF THE AMERICAN CHEMICAL SOCIETY

Article

pubs.acs.org/JACS

Catalytic Defluorination of Perfluorinated Aromatics under Oxidative Conditions Using N-Bridged Diiron Phthalocyanine

Cédric Colomban, Evgenij V. Kudrik, Pavel Afanasiev,* and Alexander B. Sorokin*

Institut de Recherches sur la Catalyse et l'Environnement de Lyon, IRCELYON, UMR 5256, CNRS − Université Lyon 1, 2 av. Albert Einstein, 69626 Villeurbanne, France

Supporting Information

ABSTRACT: Carbon−fluorine bonds are the strongest single bonds in organic chemistry, making activation and cleavage usually associated with organometallic and reductive approaches particularly difficult. We describe here an efficient defluorination of poly- and perfluorinated aromatics under oxidative conditions catalyzed by the μ-nitrido diiron phthalocyanine complex [(Pc)Fe^{III}(μ-N)Fe^{IV}(Pc)] under mild conditions (hydrogen peroxide as the oxidant, near-ambient temperatures). The reaction proceeds via the formation of a high-valent diiron phthalocyanine radical cation complex with fluoride axial ligands, [(Pc)(F)Fe^{IV}(μ-N)Fe^{IV}(F)(Pc$^{+\bullet}$)], which was isolated and characterized by UV−vis, EPR, ^{19}F NMR, Fe K-edge EXAFS, XANES, and Kβ X-ray emission spectroscopy, ESI-MS, and electrochemical techniques. A wide range of per- and polyfluorinated aromatics (21 examples), including C_6F_6, $C_6F_5CF_3$, C_6F_5CN, and $C_6F_5NO_2$, were defluorinated with high conversions and high turnover numbers. [(Pc)Fe^{III}(μ-N)Fe^{IV}(Pc)] immobilized on a carbon support showed increased catalytic activity in heterogeneous defluorination in water, providing up to 4825 C−F cleavages per catalyst molecule. The μ-nitrido diiron structure is essential for the oxidative defluorination. Intramolecular competitive reactions using $C_6F_3Cl_3$ and $C_6F_3H_3$ probes indicated preferential transformation of C−F bonds with respect to C−Cl and C−H bonds. On the basis of the available data, mechanistic issues of this unusual reactivity are discussed and a tentative mechanism of defluorination under oxidative conditions is proposed.

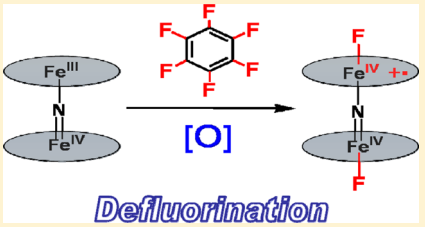

1. INTRODUCTION

Current approaches to C−F bond reactivity in organic chemistry are based on activation at electron-rich transition-metal complexes, reduction, and nucleophilic substitution.[1−4] Up to the present, fluorine chemistry has been focused on the development of synthetic methods for the preparation of various fluorous compounds, which are finding wide and increasing uses in many applications because of the unique properties of C−F bonds (C−F bond strength, high thermal and oxidative stability, low polarity, weak intermolecular interactions, etc.). In particular, the annual global production of the most important fluoroaromatics was estimated to be 35 000 tons in 2000, but the trend in the past (10 000 tons in 1994) indicates a further increase in their production and use.[5] Fluorinated compounds are particularly persistent in the environment since their biodegradation is very slow. Poly- and perfluorinated molecules are especially difficult to degrade. Consequently, along with the improvement in synthetic fluorine chemistry, the development of disposal methods for these compounds is of increasing importance. Emerging stoichiometric and rare catalytic approaches to C−F bond transformation are based on reduction.[3,6] Catalytic hydrodefluorination of aromatic fluorocarbons with alkylsilanes catalyzed by ruthenium N-heterocyclic carbene complexes under strictly anaerobic and dry conditions occurred with turnover numbers (TONs) of 1.3−7.4 for 19.45 h in the case of C_6F_6.[6c] Significant progress in the hydrodefluorination of aliphatic C−F bonds has been achieved by using carboranes in combination with alkylsilanes under an inert atmosphere in anhydrous solvents.[3,6d] These processes involving the cleavage of C−F bonds are conceived to proceed reductively. However, the use of sophisticated reagents and special conditions (dry organic solvents, inert atmosphere) compromises the practical applications of the aforementioned approaches. The development of accessible and cheap catalysts operating under practical conditions (air, water) would be a significant achievement to address emerging environmental problems due to increasing use of organofluorines and their persistence in the environment. Many biochemical aerobic processes and current depollution methods involve oxidation steps to convert recalcitrant chlorinated xenobiotics.[7] Since fluorine is the most electronegative element and C−F bonds are deactivated toward electrophilic attack,[4] the transformation of fluorinated compounds under oxidative conditions is extremely difficult and represents a fundamental challenge.

We have previously developed an iron phthalocyanine (FePc)−H_2O_2 system for the oxidative degradation of recalcitrant chlorinated phenols.[8] FePc complexes are structurally related to iron porphyrins and combine availability and high reactivity in many reactions.[9] Further development of FePc catalysts resulted in the discovery of the remarkable catalytic

Received: February 12, 2014
Published: July 17, 2014

dx.doi.org/10.1021/ja505437h | J. Am. Chem. Soc. 2014, 136, 11321−11330

properties of μ-nitrido diiron phthalocyanines.[10] The *N*-bridged diiron tetra-*tert*-butylphthalocyanine complex [(Pc)Fe^{III}(μ-N)-Fe^{IV}(Pc)] (**1**) catalyzes the oxidation of methane by H_2O_2 under mild conditions in water.[10a,b] Using the tetraphenylporphyrin (TPP) platform, we have prepared an N-bridged high-valent diiron oxo species, [(TPP)Fe^{IV}(μ-N)Fe^{IV}=O($TPP^{+\bullet}$)], that can also oxidize methane.[11] [(TPP)Fe^{IV}(μ-N)Fe^{IV}=O($TPP^{+\bullet}$)] is a much stronger oxidant than its mononuclear analogue [($TPP^{+\bullet}$)Fe^{IV}=O], and therefore, the Fe(μ-N)Fe structural feature is essential for the high catalytic activity.[11] Another example of an unusual reactivity of **1** is the formation of the high-valent [(Pc)(Cl)Fe^{IV}(μ-N)Fe^{IV}(Cl)($Pc^{+\bullet}$)] complex in the presence of ^{t}BuOOH via dechlorination of CH_2Cl_2.[10e]

Inspired by the ability of **1** to cleave C−Cl bonds in CH_2Cl_2, which is usually considered as a stable solvent for performing oxidation reactions, we checked the reactivity of other halogenated compounds in this system. Remarkably, the dehalogenation process can be extended to aromatics bearing fluorine substituents. Herein we report a highly efficient defluorination of per- and polyfluorinated aromatic compounds in the presence of N-bridged diiron phthalocyanine complex **1** and H_2O_2 that can be performed either in organic solvents or in water. A high-valent diiron intermediate involved in the catalytic cycle has been isolated and spectroscopically characterized. Mechanistic features of this unusual reactivity are discussed on the basis of ^{19}F NMR and GC−MS characterization of intermediate and final products obtained in the oxidation of several probe molecules.

2. RESULTS AND DISCUSSION

2.1. Preparation of the High-Valent Diiron Difluoro Complex in a Stoichiometric Reaction and Its Characterization. Incubation of **1** in an equimolar C_6H_6/C_6F_6 mixture in the presence of ^{t}BuOOH (30 equiv) at 60 °C for 6 h resulted in the formation of a new complex **2**, as indicated by the change in the UV−vis spectrum. The intensity of the Q band at 640 nm decreased, and new broad bands at 549, 615, and 666 nm appeared (Figure 1).

These changes are very similar to those observed during formation of [(Pc)(Cl)Fe^{IV}(μ-N)Fe^{IV}(Cl)($Pc^{+\bullet}$)] and [(Pc)-(Br)Fe^{IV}(μ-N)Fe^{IV}(Br)($Pc^{+\bullet}$)] via oxidative dehalogenation of CH_2Cl_2 and CH_2Br_2, respectively.[10e] The UV−vis spectrum of **2** is characteristic of phthalocyanine radical cations.[12] The formation of **2** from **1** led to the disappearance of the low-spin iron electron paramagnetic resonance (EPR) signal at g = 2.091 and the appearance of an intense symmetric and narrow signal (8 G width at 120 K) at g = 2.0038, typical for an organic radical (Figure 1 inset). UV−vis and EPR data suggested an Fe(IV)Fe(IV) configuration and the presence of a radical cation on one phthalocyanine ligand. Complex **2** was isolated in the solid state and further characterized. The ^{19}F NMR spectrum of **2** showed one well-defined signal at −132 ppm compatible with the presence of inorganic F^- (Figure S1 in the Supporting Information). Energy-dispersive X-ray fluorescence analysis of **2** gave a 1:1 F:Fe atomic ratio, indicating the presence of two fluoride ions per dimer molecule. The electrospray ionization mass spectrometry (ESI-MS) peak of **2** was centered at m/z 1618.5 (Figure S2). The isotopic pattern of the cluster corresponded to $(\mathbf{1} + F)^+$ formed after the loss of F^- under positive ESI-MS conditions.

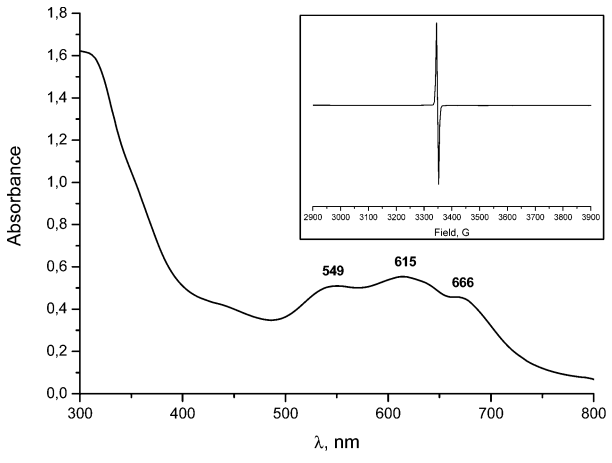

Figure 1. UV−vis spectrum of **2** obtained by the treatment of C_6F_6 with **1** and ^{t}BuOOH (MeCN, 25 °C). The inset shows the EPR spectrum of **2** in CH_2Cl_2 at 120 K (microwave frequency 9.392 GHz, power 1.6 mW, modulation 1.0 mT/100 kHz).

2.2. X-ray Absorption and Emission Spectroscopies. Core hole spectroscopies using synchrotron radiation, including extended X-ray absorption fine structure (EXAFS), X-ray absorption near-edge structure (XANES), and X-ray emission spectroscopy (XES), are widely used to determine the structures and electronic properties of enzymes and their model complexes.[13] These techniques are particularly useful for characterization of high-valent iron species.[14,15] Comparison of the Fe K-edge EXAFS spectra of the initial complex **1** and fluorine-containing species **2** shows the retention of the μ-nitrido dimer topology in **2**. However, the EXAFS spectrum of **2** was noticeably modified compared with that of the initial complex **1** (Figure 2). The changes in the EXAFS spectrum

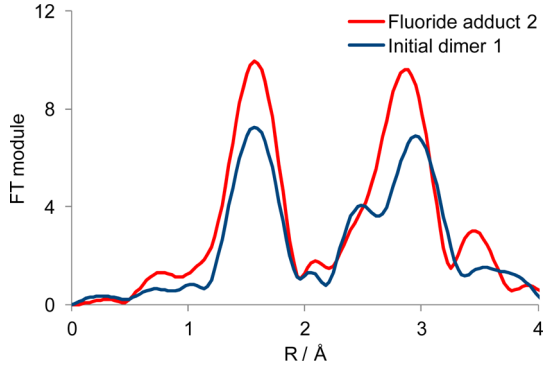

Figure 2. Fourier transforms of the EXAFS spectra of the initial complex **1** and the fluoride adduct **2**.

suggest symmetrization of the coordination environment (due to the shift of Fe atom into the plane of the macrocycle) as well as an increase in the coordination number of the iron atom.

A high-quality fit of the EXAFS spectrum of **2** for the two first coordination spheres (Figure S3 and Table S1) gave the structure shown in Figure 3, in which a fluorine ligand is bound to each iron atom at a distance of 1.99 Å, whereas other bonds distances are slightly modified relative to the initial structure of **1**, as described earlier.[10e]

In agreement with the energy-dispersive X-ray fluorescence analysis, the EXAFS spectrum of **2** indicated the presence of one F^- ion per iron atom. The Fe K-edge XANES spectra attest to a change in the oxidation state from an Fe(III)Fe(IV) core to an Fe(IV)Fe(IV) core, as indicated by a characteristic

dx.doi.org/10.1021/ja505437h | J. Am. Chem. Soc. 2014, 136, 11321−11330

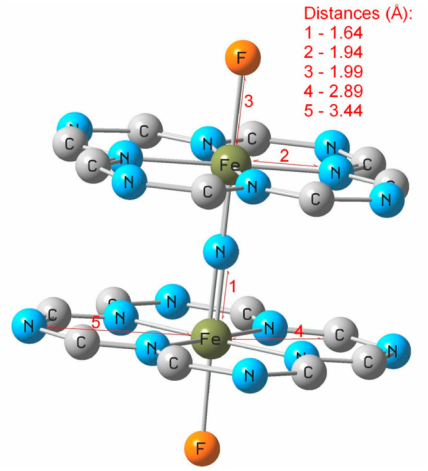

Figure 3. EXAFS structure of $[(Pc)(F)Fe^{IV}(\mu\text{-}N)Fe^{IV}(F)(Pc^{+\bullet})]$ (**2**) showing the first and second coordination spheres.

splitting of the pre-edge peak[12c] and a significant increase of the pre-edge maximum energy from 7114.7 eV in **1** to 7116.2 eV in **2** (Figure 4).

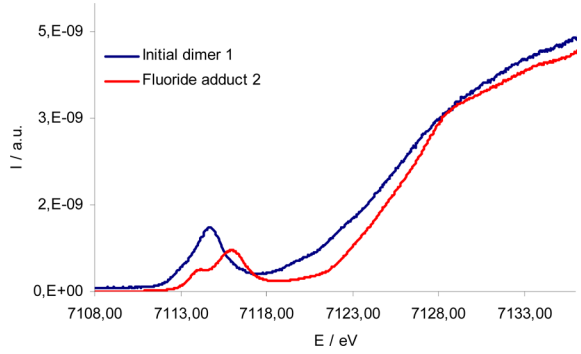

Figure 4. Fe K-edge XANES spectra of the initial $[(Pc)Fe^{III}(\mu\text{-}N)Fe^{IV}(Pc)]$ complex **1** (blue) and the $[(Pc)(F)Fe^{IV}(\mu\text{-}N)Fe^{IV}(F)(Pc^{+\bullet})]$ complex **2** (red).

Iron valence-to-core Fe Kβ XES can be used to determine light atoms within complex multimetallic strucutures.[16] For instance, this technique allowed the identification of the unique interstitial carbide ion in the iron molybdenum cofactor (FeMoco) of nitrogenase.[17] According to the Kβ XES data, **1** and **2** are both low-spin complexes. In agreement with the presence of a long Fe−F distance as determined from the EXAFS spectrum, the valence-to-core XES spectra show negligible intensity of the characteristic crossover satellite peak in the range 7075−7085 eV (Figure S4), which should clearly appear for a short Fe−F bond.

2.3. Electrochemistry. The electrochemical behaviors of **1** and **2** were investigated by cyclic voltammetry (CV) and rotating disk electrode (RDE) voltammetry in dichloromethane. The cyclic voltammogram for electrooxidation of **1** (Figure S5) displays two successive reversible one-electron oxidation waves at $E_{1/2}$ = 10 mV and $E_{1/2}$ = 400 mV relative to ferrocene/ferrocenium (Fc/Fc^+). According to RDE voltammetry experiments, both of these oxidations involve the reversible abstraction of one electron per dimer unit. These two reversible one-electron oxidations can be assigned as follows:

$$[(Pc)Fe^{III}(\mu\text{-}N)Fe^{IV}(Pc)] \rightleftarrows [(Pc)Fe^{IV}(\mu\text{-}N)Fe^{IV}(Pc)] + e^-$$

$$[(Pc)Fe^{IV}(\mu\text{-}N)Fe^{IV}(Pc)] \rightleftarrows [(Pc)Fe^{IV}(\mu\text{-}N)Fe^{IV}(Pc^{+\bullet})] + e^-$$

Electrooxidation of **2** did not show any electron-transfer process up to 1.3 V, which is consistent with the presence of the fully oxidized species $[(Pc)(F)Fe^{IV}(\mu\text{-}N)Fe^{IV}(F)(Pc^{+\bullet})]$. The CV of **2** consists of a single reversible one-electron reduction wave at $E_{1/2}$ = −385 mV vs Fc/Fc^+ (Figure S5) involving reduction by one electron per dimer unit:

$$[(Pc)(F)Fe^{IV}(\mu\text{-}N)Fe^{IV}(F)(Pc^{+\bullet})] + e^- \rightleftarrows [(Pc)(F)Fe^{IV}(\mu\text{-}N)Fe^{IV}(F)(Pc)]$$

Thus, the reduction of **2** containing coordinated fluoride anions is much more difficult (by 785 mV) than that of $[(Pc)Fe^{IV}(\mu\text{-}N)Fe^{IV}(Pc^{+\bullet})]$ containing merely perchlorate anions from the supporting tetra-*n*-butylammonium perchlorate electrolyte. This reduction potential shift is consistent with the counterion effect described for FeTPP complexes, where the reduction of (TPP)FeX undergoes a cathodic shift of up to 710 mV as the counterion is varied from weakly coordinating ClO_4^- to tightly bound F^-.[18] A spectroelectrochemical study showed the similarity of the UV−vis spectra obtained after bulk electrooxidation of **1** and reduction of **2** (Figure S6). Thus, all of the experimental data confirm the formulation of **2** as $[(Pc)(F)Fe^{IV}(\mu\text{-}N)Fe^{IV}(F)Pc^{+\bullet})]$.

2.4. Homogeneous Catalytic Oxidative Defluorination. In the presence of ^{t}BuOOH, **1** is capable of defluorinating C_6F_6 to form a binuclear $[(Pc)(F)Fe^{IV}(\mu\text{-}N)Fe^{IV}(F)(Pc^{+\bullet})]$ complex. This complex is stable under the reaction conditions, and no further defluorination occurs. Clearly, **1** shows a very intriguing defluorination ability, though with ^{t}BuOOH the process is not catalytic but instead is a stoichiometric reaction. However, if **2** could be reduced back to **1**, a fascinating possibility would arise for the mild catalytic defluorination. Our attempts to find a catalytic pathway led to success. Upon interaction of **2** with H_2O_2, we observed the transformation of **2** to the initial **1** via a yet-unknown intermediate **3** showing a peak at λ = 617 nm in the UV−vis spectrum. Assuming that the defluorinations in the presence of H_2O_2 and ^{t}BuOOH proceed similarly, we propose the catalytic cycle shown in Figure 5.

To demonstrate the possibility of a catalytic cycle, we treated 0.1 M pentafluorophenol solution with H_2O_2 (16 equiv) in the presence of 0.4 mol % catalyst **1** in MeCN at 60 °C in a Teflon reactor. ^{19}F NMR analysis of the reaction mixture after 15 h showed 82% C_6F_5OH conversion and the formation of 4.0 F^- (mostly in the form of HF) per one converted C_6F_5OH molecule. A high TON (i.e., moles of F^- formed per mole of catalyst) of 818 was achieved. When the reaction was performed in a glass flask, a significant amount of hexafluorosilicate was isolated (as shown by ^{19}F NMR and IR data), thus confirming the formation of HF during the reaction. It is noteworthy that the **1**−H_2O_2 system efficiently performs defluorination of C_6F_5OH even at 20 °C, with 88% conversion after 24 h.

The reaction was further extended to a large scope of substrates (Figure 6). Even hexafluorobenzene, pentafluoropyridine, and octafluoronaphthalene as well as polyfluorinated aromatic compounds containing functional groups were

dx.doi.org/10.1021/ja505437h | J. Am. Chem. Soc. 2014, 136, 11321−11330

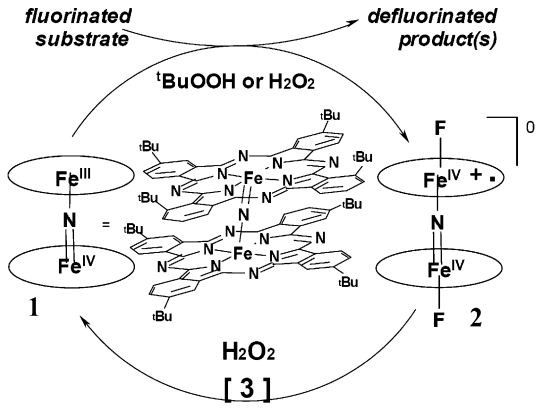

Figure 5. Structure of N-bridged diiron tetra-*tert*-butylphthalocyanine complex **1** and proposed catalytic cycle for oxidative defluorination. The ovals stand for the tetra-*tert*-butylphthalocyanine ligand.

transformed with high TONs. High degrees of defluorination in terms of the number of F^- ions formed per converted substrate molecule were achieved. From six fluorine atoms of C_6F_6, 3.12 were transformed to inorganic F^-. The presence of strong electron-withdrawing substituents (CN, NO_2) was tolerated. No products of transformation of the CF_3 group were found in the course of oxidation of octafluorotoluene. The oxidation of octafluoronaphthalene afforded heptafluoronaphthols, hexafluoro-1,4-naphthoquinone, tetrafluorophthalic acid, difluoromaleic acid, and difluorofumaric acid.

2.5. Heterogeneous Catalytic Defluorination in Water. It should be noted that defluorination reactivity of **1** was observed in acetonitrile, which can also be oxidized under the reaction conditions.[10a] The concurrent solvent oxidation can partially hide the real performance of **1** in the defluorination of recalcitrant fluoroaromatics. The best way to avoid side reactions involving organic solvents is to use water, a green and stable solvent. To this aim, complex **1** was supported on carbon (**1**-C, 300 m^2/g BET surface area, 10 μmol/g), and heterogeneous defluorination reactions were carried out in water. The catalytic system was not deactivated in aqueous solution, and high performance of the supported catalyst **1**-C was observed in the transformation of fluorinated compounds (Figure 7).

In water, 4825 C−F bonds of C_6F_5OH per catalyst molecule were mineralized with the release of F^-. C_5F_5N and C_6F_6, which are only sparingly soluble in water, were transformed with 85% and 75% conversion, respectively, indicating a high catalytic performance even in dilute solutions. This tolerance to water is of exceptional importance since other approaches to defluorination often need anhydrous conditions.[6]

The efficiency of mineralization depends on the H_2O_2:substrate ratio. Quasi-complete conversion of C_6F_5OH with 70−80% mineralization was achieved using 10−26 equiv of H_2O_2. The kinetics of the oxidative degradation of C_6F_5OH at 60 °C in the presence of **1**-C (0.1 mol %) and H_2O_2 (26 equiv) was monitored by ^{19}F NMR spectroscopy (Figure 8). The signals of C_6F_5OH at −163.3, −165.6, and −170.7 ppm progressively disappeared, showing conversions of 37%, 51%, and 96% after 2.5, 5, and 15 h, respectively. The main reaction products were DF, oxalic acid, and difluoromaleic acid as well as a small amount of fluorooxaloacetic acid [as confirmed by GC−MS after methylation with $(CH_3)_3SiCHN_2$]. The yields of the final products of the C_6F_5OH transformation are shown in Figure 9.

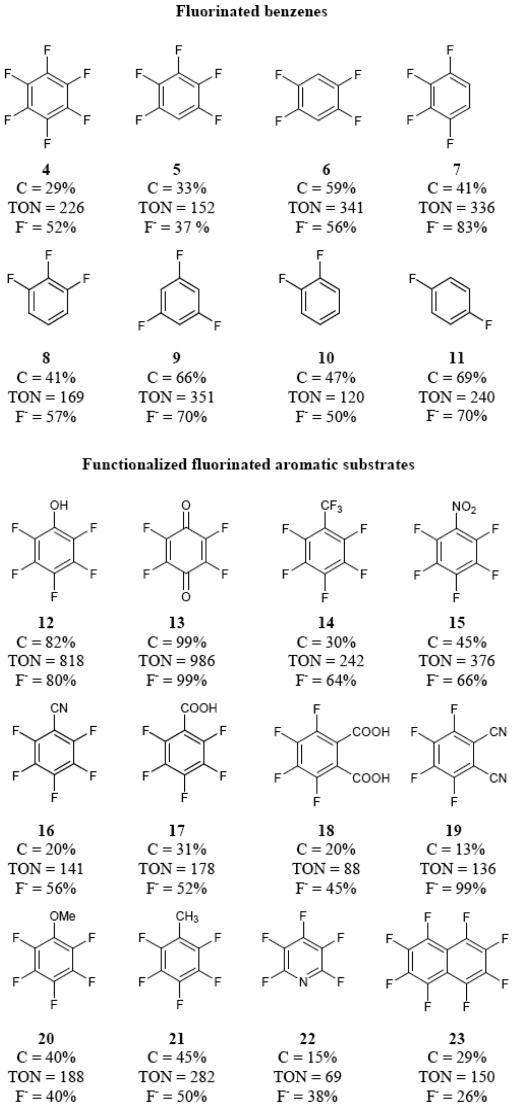

Figure 6. Scope of the catalytic homogeneous dehalogenation of polyfluorinated aromatics by the **1**−H_2O_2 system. The solution containing the catalyst (0.4 mM), substrate (0.1 M), and H_2O_2 (1.6 M) was stirred in CD_3CN at 60 °C for 15 h. The catalyst:substrate:oxidant ratio was 1:250:4000. The substrate conversions (C) and yields of F^- were determined by ^{19}F NMR spectroscopy. Turnover numbers (TONs) were calculated as the molar amount of F^- formed per mole of the catalyst. The degree of defluorination (F^-) is the ratio of the amount of F^- formed to the total amount of fluorine in the converted substrate.

The total organic carbon analyses showed a 53.6% loss of the organic carbon due to the formation of CO_2 and CO, which were identified in the gas phase in a 15:1 ratio. Importantly, 89% of the organic fluorine was transformed to inorganic fluoride anions. These results indicate a very efficient mineralization of the water-soluble fluorinated aromatics using the heterogeneous catalyst in combination with clean H_2O_2 oxidant in water without any additives.

2.6. Preparative Oxidative Defluorination. Smaller excesses of H_2O_2 led to more selective reactions. With 5 equiv of H_2O_2, a 62% yield of difluoromaleic acid and a 66% yield of tetrafluorophthalic acid were obtained during the transformations of C_6F_5OH and octafluoronaphthalene, respectively (Figure 10). Thus, the **1**−H_2O_2 catalytic system

dx.doi.org/10.1021/ja505437h | J. Am. Chem. Soc. 2014, 136, 11321−11330

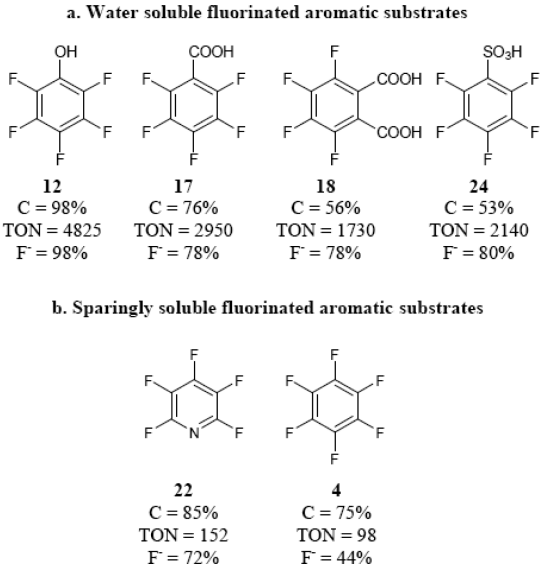

Figure 7. Catalytic heterogeneous dehalogenation of polyfluorinated aromatics by the **1**-C−H_2O_2 system. Reactions were run by stirring the supported catalyst (20 mg, 0.2 μmol of complex), substrate [(a) 0.1 M; (b) 0.005 M for C_5F_5N and 0.003 M for C_6F_6], and H_2O_2 [(a) 2.6 M; (b) 0.1 M] in D_2O at 60 °C for 15 h. The catalyst:substrate:oxidant ratio was 1:1000:26000 in (a) and 1:50:1000 for C_5F_5N and 1:96:3200 for C_6F_6 in (b).

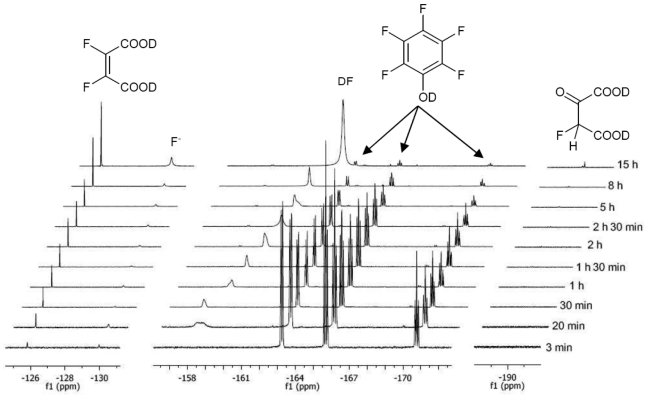

Figure 8. Kinetics of C_6F_5OH degradation and formation of oxidation products. The time dependence of the ^{19}F NMR spectra shows the oxidative degradation of 0.1 M C_6F_5OH at 60 °C in D_2O performed under the conditions described in Figure 7.

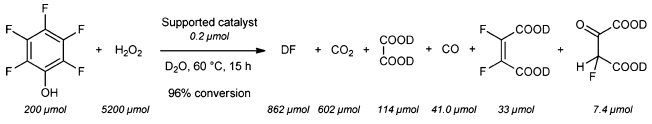

Figure 9. Yields of the final products of the C_6F_5OH transformation. The fluorine and carbon amounts found in the products represented 97% and 89%, respectively, based on the substrate content.

can be also adapted for the preparation of functionalized fluorinated molecules from available poly- and perfluoroaromatic compounds.

2.7. Study of the Reactivity of Fluoroaromatics Using Other Systems. The reactivities of monomeric $FePc^tBu_4(Cl)$ toward C_6F_5OH and C_6F_6 were checked under the same conditions (CD_3CN, 60 °C, 15 h). Importantly, no conversion of C_6F_6 was detected with $FePc^tBu_4(Cl)$. The $FePc^tBu_4(Cl)$

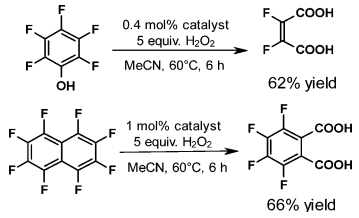

Figure 10. Preparative oxidations of pentafluorophenol and octafluoronaphthalene using the **1**−H_2O_2 system.

showed a low catalytic activity only toward C_6F_5OH. A 23% conversion of C_6F_5OH, a TON of 160, and 56% mineralization were obtained with $FePc^tBu_4(Cl)$, compared with 82% conversion, a TON of 818, and 80% mineralization observed in the presence of **1**. Therefore, the dimeric strucure of **1** is essential for the high defluorination activity. μ-Oxo and μ-carbido diiron phthalocyanine complexes were not active toward C_6F_6, indicating the essential role of the Fe(μ-N)Fe structural unit. Previously, a pronounced axial ligand effect on oxidation activity was observed for iron porphyrin complexes.[19] The influence of the axial ligand was explained by its electron donor effect and by the stabilization of the final catalyst state, thus modulating the reaction free energy for epoxidation, hydrogen atom abstraction, or demethylation. In single-atom-bridged diiron complexes (μ-oxo, μ-nitrido, μ-carbido), the nature of the bridging ligand seems to be even more important. μ-Nitrido diiron species exhibit a reactivity that other complexes do not show. Further experimental and calculation studies are necessary to understand the reason(s) for the unprecendented reactivity of μ-nitrido diiron complexes.

Early reports showed that hydroxyl radicals generated by thermal decomposition of H_2O_2 can react with octafluoronaphthalene and heptafluoronaphthols to form dimeric coupling products and hexafluoronaphthoquinone.[20] Photo-Fenton defluorination of C_6F_5OH and C_6F_5COOH using ferrous sulfate or ferric oxalate in combination with H_2O_2 and UV-C light (200−300 nm) has been reported.[21] However, it has been shown that C_6F_6 does not react with $OH^\bullet$ radicals generated by thermolysis of 90% H_2O_2 in acetonitrile even at 100 °C.[22] To verify the possible involvement of Fenton chemistry, we tested the reactivities of 15 fluorinated substrates in the presence of $FeSO_4$ and H_2O_2 under the conditions used for the **1**−H_2O_2 system. The only substrate that exhibited similar reactivities with **1** and $FeSO_4$ was fluoranil. Importantly, all of the fluorinated benzenes from $C_6H_4F_2$ to C_6F_6 remained completely unchanged under Fenton conditions. The substrates containing electron-donating (**12**, **20**, and **21**) or electron-withdrawing substituents (**14**−**19**) showed conversions at the detection limit. When the $FeSO_4$ loading was increased 25 times (to 10 mol %), C_6F_6 (0.1 M in CD_3CN) did not react with H_2O_2 (1.6 M) at 60 °C for 15 h. These results indicate that hydroxyl radicals should not be responsible for the oxidative defluorination of fluorinated aromatic compounds catalyzed by **1**.

To probe the stabilities of the substrates and identified intermediates under the reaction conditions, control experiments were performed without the catalyst under the same reaction conditions in CD_3CN and D_2O. With all of the studied substrates, including C_6F_5OH (an intermediate in the degradation of C_6F_6), no reaction was observed. The only exception was found for tetrafluoro-1,4-benzoquinone, which was capable of reacting with H_2O_2 to form trifluorohydroxy-*p*-

dx.doi.org/10.1021/ja505437h | J. Am. Chem. Soc. 2014, 136, 11321−11330

benzoquinone.[23] The treatment of fluoranil (0.1 M in CD_3CN) with H_2O_2 (1.6 M) for 15 h at 60 °C led to 89% substrate conversion. However, the reaction without catalyst was slower than catalytic reaction (29% vs 56%, respectively, after 30 min). The noncatalyzed reaction was less efficient than the catalytic process in terms of degree of defluorination (2.00 F^- vs 4.00 F^- formed per converted substrate, respectively). All of these results indicate the essential role of the μ-nitrido diiron complex in defluorination of fluorinated aromatics under oxidative conditions.

2.8. Comparison of the Reactivities of the 1−H_2O_2 System toward C−F, C−Cl, and C−H Bonds. The relative reactivity of C−F bonds versus C−Cl and C−H bonds was evaluated using an intramolecular competitive approach. The oxidation of several substrates employed in a large excess was monitored at short reaction times in order to determine the initial reaction products (Figure 11). The dehalogenation of

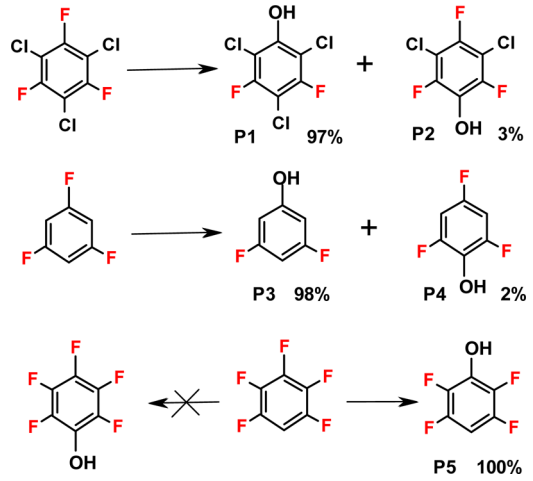

Figure 11. Relative reactivities of C−F bonds vs C−Cl and C−H bonds determined in intramolecular competition reactions. The ratios of phenols were determined after 1 h. Only the major product **P5** is shown for the transformation of pentafluorobenzene.

1,3,5-trichloro-2,4,6-trifluorobenzene ($C_6F_3Cl_3$) resulted in the formation of phenol **P1** (F elimination) and phenol **P2** (Cl elimination) in a ratio of ~97:3. The transformation of 1,3,5-trifluorobenzene yielded phenol **P3** (F elimination) and phenol **P4** (C−H oxidation) in a ratio of ~98:2. Remarkably, only tetrafluorophenols (F elimination) were obtained in the reaction with pentafluorobenzene. No traces of pentafluorophenol resulting from C−H oxidation were detected. Although these phenols are the intermediate products and these ratios might slightly deviate from the ratios of the intrinsic reactivities of C−F versus C−Cl and C−H bonds, the results obtained clearly show an unusually strong preference of the catalytic system for the transformation of C−F bonds with respect to C−Cl and C−H bonds. Such unusual selectivity gives an indirect indication that the initial reaction step involves a transformation of a C−F bond.

2.9. Mechanistic Considerations. *2.9.1. General Remarks.* The counterintuitive defluorination of aromatic C−F bonds under oxidative conditions and preferential defluorination versus dechlorination and oxidation of C−H bonds demonstrated by **1** raise questions about the possible mechanistic background of this striking reactivity. In this section, we discuss several possible scenarios of oxidative defluorination of fluoroaromatics by **1** and provide preliminary considerations regarding the possible mechanism. Available EXAFS, XANES, ESI-MS, Mössbauer, EPR, labeling, and reactivity data indicate the involvement of hydroperoxo and high-valent diiron oxo species in the 1−H_2O_2 system,[11,12c] showing mechanistic features similar to those of biological oxidation [e.g., intermediate formation of benzene epoxide and the occurrence of a 1,2-shift (NIH shift) during oxidation of benzene].[10c] However, no biodegradation of perfluorinated compounds has ever been reported,[24] and experimental studies on the oxidation of highly halogenated aromatics containing fluorine substituents are rare.[25] On the basis of the available data, we consider below several mechanistic hypotheses.

2.9.2. Nucleophilic Substitution Hypothesis. S_NAr nucleophilic attack on C−F bonds mediated by transition-metal complexes (Pd, Rh, Ni, etc.) or oxidative addition of C−F bonds may result in the formation of C−X bonds (X = H, N, O, S).[26] However, all reported cases of such C−F bond substitution occur under basic conditions and/or on electron-rich transition-metal complexes, which is not the case for **1**. In general, the higher reactivity of the C−F bond compared with the C−Cl bond in the transformation of $C_6F_3Cl_3$ is compatible with a nucleophilic mechanism since the reactivity of the aryl halides decreases in the order of F > Cl > Br > I.[1] However, the conversions of fluorinated benzenes are higher for less-fluorinated compounds: C_6F_6 (29%), C_6F_5H (33%), 1,2,4,5-$C_6F_4H_2$ (59%), 1,3,5-$C_6F_3H_3$ (66%), 1,4-$C_6F_2H_4$ (69%). Similarly, the conversions of substrates with one electron-withdrawing group are higher than those of substrates bearing two such groups: $C_6F_5(COOH)$ (52%) versus $C_6F_5(COOH)_2$ (20%) and $C_6F_5(CN)$ (20%) versus $C_6F_5(CN)_2$ (13%). A competition reaction between $C_6F_5CF_3$ and $C_6F_5CH_3$ resulted in conversions of 31% and 49%, respectively, while $C_6F_5CF_3$ and $C_6F_5CH_3$ show similar reactivities in S_NAr reactions.[27] Although on the basis of these reactivity trends a nucleophilic substitution mechanism cannot be definitively excluded, the observed results seem to be better compatible with the participation of electrophilic species.

2.9.3. Electrophilic Attack Hypothesis. High-valent iron oxo species are potent oxidants and possess strong electrophilic properties. However, the observed preference for cleavage of C−F bonds versus C−H and C−Cl bonds is not compatible with an initial direct electrophilic attack of a high-valent diiron oxo species on the C−X bond (X = F, Cl, H) because in this case the more electron-rich C−H or C−Cl bonds should be preferred. On the other hand, in vitro and in vivo cytochrome P-450-dependent biotransformations of C_6F_5Cl and $C_6F_3Cl_3$ exhibited the preferential elimination of the *p*-F substituent and formation of **P1**, respectively.[25] Calculations predicted a higher reactivity of the *p*-F position of C_6F_5Cl and a fluorinated position of $C_6F_3Cl_3$. A density functional theory (DFT) study showed that activation of C_6F_6 proceeded by π attack of Compound I on the aromatic ring to form hexafluorocyclohexadienone with a lower activation barrier compared with that for C_6Cl_6.[7] The intermediate formation of cyclohexadienone species from arene epoxides has been postulated in numerous studies on hydroxylation of aromatic compounds.[28]

2.9.4. Initial Epoxidation Step. Aromatic oxidation performed by cytochrome P-450 involving high-valent iron oxo species leads to intermediate formation of arene epoxides accompanied by NIH shifts.[28] Epoxide intermediates were also proposed to be the primary metabolites in cytochrome P450-catalyzed oxidation of halobenzene derivatives.[29] In turn, the

dx.doi.org/10.1021/ja505437h | J. Am. Chem. Soc. 2014, 136, 11321−11330

oxidation of benzene by the **1**−H_2O_2 system was shown to occur via the initial formation of benzene epoxide.[10c] Consideration of the shapes and energies of the lowest unoccupied molecular orbital (LUMO) and highest occupied MO (HOMO) of C_6F_5H suggests that initial epoxidation should occur on the CF═CF bond rather than on the CH═CF bond, in agreement with the observed selectivity. Moreover, the observed higher reactivity of C_6F_5H versus C_6F_6 also agrees with the relative energy of the HOMOs (see Figure S7 and the attached comment). Thus, the hypothesis of the initial formation of the fluoroarene epoxide seems to be plausible. Up to now, our attempts to detect the putative hexafluorobenzene epoxide have been unsuccessful, probably because of its low stability under the high temperatures of GC−MS analysis. The low response of fluorinated compounds under ESI-MS conditions also prevents the application of this technique for detection of epoxides of fluoroarenes. Nevertheless, when octafluoronaphthalene was used as the substrate, GC−MS analysis of the reaction mixture showed the presence of a minor product with a signal at m/z 288 corresponding to $C_{10}F_8O$ formulation, which can only be attributed to epoxide. The fragmentation pattern of this product is also compatible with an octafluoronaphthalene epoxide structure (Figures S8−S13).

The initial epoxide formation can be also proposed upon the detection of the NIH shift (migration of the substituent to an adjacent position).[10c,28,30] The NIH shift was evidenced for chlorinated and brominated aromatics,[31] but the migration of fluorine is far less documented.[32] The fluorine substituent is preferentially eliminated from an aromatic molecule rather than giving rise to an NIH shift.[29]

Several fluorobenzenes have been tested in the search of the fluorine NIH shift. The occurrence of this phenomenon in P-450-catalyzed oxidation was evidenced using 1,4-difluorobenzene.[30] We applied the same approach to probe the fluorine NIH shift in our system. Along with *p*-fluorophenol as a major product, the oxidation of 1,4-difluorobenzene using the **1**−H_2O_2 system did lead to the formation of the NIH-shifted 2,4-difluorophenol along with 2,5-difluorophenol (the normal oxidation product) in a ratio of ∼1:15 (Figure 12). The

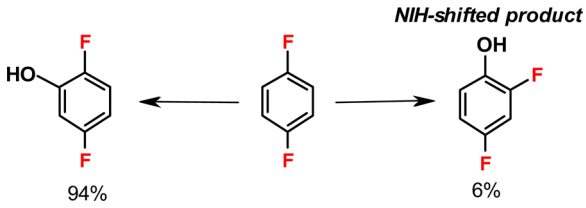

Figure 12. Initial products of the 1,4-difluorobenzene transformation in the presence of **1** and H_2O_2. Conditions: MeCN, 60 °C. The ratios of phenols were determined after 25 min.

detection of the fluorine NIH shift is in agreement with the involvement of the epoxidation as an initial step of the oxidative defluorination of poly- and perfluorinated aromatics.

2.9.5. Tentative Mechanism of Defluorination under Oxidative Conditions. It is thus conceivable that the first step of defluorination could involve epoxidation of a fluorinated aromatic molecule by [Fe^{IV}(μ-N)Fe^{IV}═O phthalocyanine radical cation]^0 species. RI-PBE and B3LYP DFT calculations showed the feasibility of this mechanism for cytochrome P450 Compound I.[7] In our case, [Fe^{IV}(μ-N)Fe^{IV}═O phthalocyanine radical cation]^0 species capable of oxidizing methane[10a] might also be competent to attack fluoroaromatics. Alternatively, the previously identified hydroperoxo complex [(Pc)Fe^{IV}(μ-N)-Fe^{III}(Pc)(OOH)] formed from **1** and H_2O_2 in the initial step of H_2O_2 activation[10e] could also be responsible for the epoxidation of fluorinated aromatics. The epoxidation of electron-deficient olefins by nucleophilic monoferric porphyrin peroxo complexes has been reported,[33] providing support for this scenario.

A reaction pathway for the oxidative defluorination of C_6F_6 is proposed in Figure 13. The epoxide of the fluoroarene undergoes a transformation to phenol via the formation of the ketone intermediate. This mechanism giving rise to the NIH shift is well-established for the oxidation of aromatic compounds by high-valent iron oxo species.[28] The fluorine NIH shift detected in the oxidation of *p*-$C_6H_4F_2$ strongly suggests a similar mechanism for the transformation of fluoroarenes. The further oxidation of C_6F_5OH results in the formation of fluoranil, which was identified by GC−MS and ^{19}F NMR analyses. The well-documented oxidation of halogenated phenols to quinones catalyzed by cytochrome P-450[7,25,28] and phthalocyanine complexes[8] supports this mechanism. The high degrees of defluorination observed in the transformations of fluoroarenes imply cleavage of the aromatic cycle with further formation of F^-. We assume that fluoranil can be further epoxidized, with subsequent hydrolysis of the epoxide and elimination of HF according to the mechanism for degradation of chlorinated quinones proposed in ref 8b. The fluorinated quinone can also undergo a nucleophilic attack by the peroxo complex at the electron-deficient carbonyl position, resulting in cleavage of the aromatic cycle and formation of oxalic and maleic acids similar to the mechanism proposed for the degradation of chlorinated phenols.[8] The degradation of fluoranil in the presence of nucleophilic H_2O_2 is in agreement with this mechanism. Further epoxidation and C−C bond cleavage steps lead to the formation of HF and CO_2. Difluoromaleic, fluorooxaloacetic, and oxalic acids as well as CO_2 and CO have been identified by GC−MS and ^{19}F NMR techniques (Figures S14−S17).

The proposed reaction pathway where numerous intermediate and final products have been identified (shown in red in Figure 13) is compatible with all of the available experimental data. However, further experimental and theoretical studies are still necessary to gain deeper insights into the mechanism of defluorination of aromatic compounds under oxidative conditions.

3. CONCLUSION

Although there are a variety of efficient systems for C−F activation based on electron-rich organometallic complexes, reduction, and nucleophilic substitution, the oxidative transformations of poly- and perfluorinated compounds are practically unknown in chemistry and biology. In this context, the discovery and development of a novel route for the activation of C−F bonds would be of the utmost importance. We have found that a μ-nitrido diiron phthalocyanine complex reacts with C_6F_6 in the presence of peroxides. Using ^{t}BuOOH we have prepared the high-valent diiron complex [(Pc)(F)-Fe^{IV}(μ-N)Fe^{IV}(F)($Pc^{+\bullet}$)] with two fluoride ligands originating from the cleavage of aromatic C−F bonds. This complex was characterized by UV−vis, EPR, ^{19}F NMR, Fe K-edge EXAFS, XANES, and Kβ X-ray emission spectroscopy, ESI-MS, and electrochemical techniques. This stoichiometric chemistry was further developed into a catalytic version. The first catalytic

dx.doi.org/10.1021/ja505437h | J. Am. Chem. Soc. 2014, 136, 11321−11330

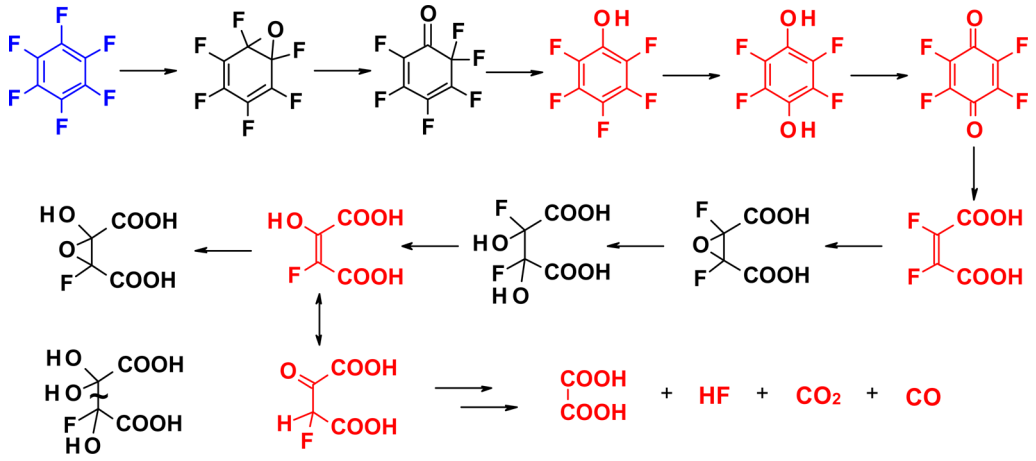

Figure 13. Proposed reaction pathway for oxidative defluorination of hexafluorobenzene in the presence of **1**. Identified intermediates and final products are shown in red.

system for the efficient defluorination of poly- and perfluorinated aromatics under oxidative conditions is based on the μ-nitrido diiron phthalocyanine complex and H_2O_2. A variety of poly- and perfluorinated aromatic compounds (21 examples) were defluorinated with high turnover numbers, showing the large substrate scope of this approach. The mechanistic basis of this unprecedented reactivity is of great interest since the oxidative transformation of heavily fluorinated compounds has been considered as almost impossible. A tentative mechanism has been proposed on the basis of available data, but further experimental and theoretical studies are necessary to provide deeper insights. We believe that this novel approach to the transformation of C−F bonds has fundamental character with a great potential for further development. In addition, this unexpected reactivity might be used in practical applications, such as the disposal of fluorinated compounds. In fact, the large-scale production and application of fluorinated xenobiotics (40% of agrochemicals and 20% of pharmaceuticals currently used contain C−F bonds[2]) coupled with their exceptional stability lead to their accumulation in the environment with the risks of contamination of the food chain and ground and drinking water.[34] Poly- and perhalogenated aromatics are among the most recalcitrant pollutants. The development of practical disposal methods for these contaminants of emerging concern is therefore of great importance.[5] Reductive hydrodefluorination of organofluorines as proposed in the literature is usually performed under anaerobic and dry conditions.[6] The only exception is the preparative reductive hydrodefluorination using Zn in concentrated ammonia solutions.[35] However, any practical applications of these reductive methods for remediation can hardly be envisaged. In contrast, the N-bridged diiron phthalocyanine complex in combination with H_2O_2 reacts with aromatic C−F bonds in water under near-ambient conditions. In this context, the proposed oxidative approach seems to be particularly promising. Indeed, (i) the iron catalyst is nontoxic and cheap and can be available on a large scale; (ii) H_2O_2 is a green and cheap industrial oxidant; (iii) the catalytic system shows a large substrate scope and is tolerant to water and air; (iv) the process can be performed in concentrated solutions (typically the case of industrial wastes) or in dilute aqueous solutions (treatment of contaminated water). For all of these reasons, this novel fundamental approach to the activation of C−F bonds can be developed for the degradation of fluorinated pollutants that are resistant to biodegradation and traditional remediation methods.

4. EXPERIMENTAL SECTION

4.1. Equipment and Methods. Mass spectra were acquired on a ThermoFinnigan LCQ Advantage ion trap instrument, detecting positive ions (+) or negative ions (−) in the ESI mode. Liquid-state ^{1}H and ^{19}F NMR spectra were obtained using a Bruker AM 250 spectrometer. Solid-state ^{19}F NMR spectra were acquired on a Bruker DSX 400 spectrometer. The UV−vis spectra of solutions were obtained with an Agilent 8453 diode-array spectrophotometer. The reaction products were identified by GC−MS [Hewlett-Packard 5973/6890 system; electron impact ionization at 70 eV, He carrier gas, 30 m × 0.25 mm HP-INNOWax capillary column with poly(ethylene glycol) (0.25 μm coating) or DB-5MS 50 m capillary column (0.250 mm × 0.25 μm)]. The reaction products were analyzed using The NIST Mass Spectral Search Program of NIST/EPA/NIH Mass Spectral Library (version 2.0f, July 23, 2008). In order to analyze organic acids, reaction mixtures were treated with a 2.0 M solution of (trimethylsilyl)diazomethane in diethyl ether to transform caboxylic groups to the methyl esters. Response factors of phenol products were determined using authentic compounds. When authentic compounds were not available, phenol products were analyzed by assuming that they have the similar response factors as their available isomers. Total organic carbon analyses were performed on a Shimadzu TOC-5050A spectrometer. Infrared spectra were recorded on a Bruker Vector 22 FTIR spectrometer using KBr pellets. EPR spectra were recorded on a Bruker Elexsys e500 spectrometer (conditions: 25 °C, microwave frequency 9.415 GHz, power 0.4 mW, modulation 1.0 mT/100 kHz).

X-ray emission spectra were measured at beamline ID 26 at the European Synchrotron Radiation Facility (ESRF) (Grenoble, France). The electron energy was 6.0 GeV, and the ring current was varied from 50 to 90 mA. Two u35 undulators were used to perform the measurements. To detect the (resonant) inelastic X-ray scattering, the sample pellet was aligned at an angle of 45° with respect to the X-ray beam. The incident X-ray energy was selected by a pair of Si crystals cut in the (220) orientation. The beam was focused in a small spot (350 μm × 60 μm) on the sample. The scattered X-rays were monochromatized by the (531) Bragg planes of a spherical bent Si crystal and focused on an avalanche photodiode (APD). When the energy of the scattered X-rays was scanned, the APD detector and the spherical bent Si crystal were moved concertedly in order to keep the beam spot on the sample, the bent crystal, and the detector on a Rowland circle. A He bag was fixed between the sample, analyzer crystal, and detector in order to minimize the absorption of the X-rays by air. In order to minimize radiation damage, the samples were cooled to a temperature in the range 20−30 K, and the position of the beam on the sample was changed regularly between scans. In order to be

dx.doi.org/10.1021/ja505437h | J. Am. Chem. Soc. 2014, 136, 11321−11330

sure that the X-ray beam did not destroy the iron species under study, we checked the absence of radiation damage during the exposure time. To do this, prior to every measurement, 30 scans were performed (30 s each), and XANES profiles were detected. The absence of evolution within the series of subsequent XANES spectra was applied as a criterion of stability under the beam.

The EXAFS and XANES spectra were recorded on the SAMBA beamline at the SOLEIL synchrotron (Gif-sur-Yvette, France) operating at 300 mA and 2.75 GeV. Spectra were collected in transmission mode at the Fe K edge with a sagittal focusing Si(220) double crystal and focusing mirrors graded at 5 mrad to remove the harmonics. The beam spot was defocused to prevent beam damage to the sample. To compare the pre-edge energies, a metallic Fe foil reference was applied. The first inflection point of metallic Fe was observed at 7111.6 eV. The data were treated with the FEFF[36] and VIPER[37] programs, and then the edge background was extracted using Bayesian smoothing with a variable number of knots. The curve fitting was done alternatively in the R and k spaces, and the fit was accepted only in the case of simultaneous convergence in k and R spaces (absolute and imaginary parts for the latter). The coordination numbers (CN), interatomic distances (R), Debye−Waller (DW) parameters (σ^2), and energy shifts (ΔE_0) were used as fitting variables. Constraints were introduced on the variables such as DW factors and energy shifts to get values lying in physically reasonable intervals. Constraints imposed by the molecular structure were also introduced. The quality of the fit was evaluated using the values of variance and goodness.

4.2. Determination of Substrate Conversions and Product Yields by ^{19}F NMR Spectroscopy. The disappearance of fluorinated substrates and the appearance of fluorinated products were determined by ^{19}F NMR spectroscopy using a hexafluoroisopropanol solution in CD_3CN as an external standard in a sealed capillary placed in an NMR tube or CF_3COOH as an internal standard. Prior to analyses of the products of catalytic reactions, calibration was performed with solutions of KF in D_2O and solutions of hexafluorobenzene in CD_3CN. In both cases, the integration values linearly depended on the KF and C_6F_6 concentrations. The signal intensities of inorganic and organic fluorine atoms were identical. In some experiments performed in water, CF_3COOH was used as a standard. The total mass balance for fluorine was >90% by ^{19}F NMR spectroscopy. Hydrofluoric acid is a weak acid and is present in dilute aqueous solutions in nonionized and ionized forms showing two ^{19}F NMR signals. On the basis of literature data, a signal at −129.9 ppm was assigned to F^-. This assignment was confirmed by measurement of the ^{19}F NMR spectrum of a KF solution in D_2O, which showed the signal with the same chemical shift. This signal was observed only using D_2O solvent. When the reactions were performed in CD_3CN, this signal was absent. A broad peak at approximately −160 ppm was assigned to hydrated nonionized HF. Concentrations of fluoride ion were additionally determined by a spectrophotometric method according to a published protocol.[38] The fluoride ion concentrations determined by the two methods were the same within experimental errors of 5−10%.

4.3. Determination of Gas-Phase Products by the Micro-GC−MS Method. Typical amounts of the supported catalyst, pentafluorophenol, and H_2O_2 were placed in a Schlenk tube under an argon atmosphere, and the gas phase was immediately analyzed by the micro-GC−MS method. CO was not detected, whereas the background content of CO_2 was equal to 0.15%. The reaction mixture was stirred under argon at 60 °C for 15 h. The analysis of the gas phase after reaction showed 48.18% CO_2 content and 3.27% CO content.

4.4. Preparation of Catalysts. Tetra-*tert*-butylphthalocyaninatoiron(II) was synthesized and purified according to a published protocol.[39] μ-Nitridobis(tetra-*tert*-butylphthalocyaninatoiron), $(FePc^tBu_4)_2N$, was prepared as described previously.[10a] The supported catalyst was prepared as follows: $(FePc^tBu_4)_2N$ (80 mg, 50 μmol) was dissolved in 200 mL of CH_2Cl_2, and 5 g of carbon (HSAG 300, specific surface area 300 m^2/g) was added to the solution. The resulting mixture was stirred for 6 h at room temperature, and the solvent was evaporated under reduced pressure. The solid material was dried in vacuum at room temperature for 1 h and at 60 °C for 6 h. The complex loading was 10 μmol/g.

4.5. Preparation of the μ-Nitrido Diiron(IV) Tetra-*tert*-butylphthalocyanine Difluoride Complex. μ-Nitrido diiron *tert*-tetrabutylphthalocyanine (16 mg) was dissolved in 10 mL of a 1:1 C_6H_6/C_6F_6 mixture. After addition of a 70% aqueous solution of tBuOOH (40 μL, 30 equiv with respect to the complex), the reaction mixture was stirred at 60 °C for 6 h. The solvent was removed, and the isolated product was washed with water and dried at 60 °C in vacuum. The yield of the dark-blue powder was 13 mg (80%).

4.6. Typical Procedures for Oxidative Defluorination. *4.6.1. Homogeneous Oxidation in Acetonitrile.* A 3 mL Teflon reactor was charged with 2 mL of CD_3CN containing polyfluorinated substrate (0.1 M), H_2O_2 (typically 1.6 M), and catalyst (0.4 mM). The reactor was kept at the desired temperature (20 or 60 °C) with magnetic stirring for 1, 3, 6, or 15 h. After cooling to room temperature, the reaction mixture was analyzed by GC−MS and ^{19}F NMR methods.

4.6.2. Homogeneous Oxidation under Fenton Conditions. A 3 mL Teflon reactor was charged with 2 mL of CD_3CN or D_2O containing fluorinated substrate (0.1 M), H_2O_2 (1.6 M), and a 4 mM solution of iron(II) sulfate dihydrate in water (0.4 mM). The reactor was kept at 60 °C with magnetic stirring for 15 h. After cooling to room temperature, the reaction mixture was analyzed by the ^{19}F NMR method.

4.6.3. Heterogeneous Oxidation in Water. A 3 mL Teflon reactor was charged with 2 mL of D_2O containing polyfluorinated substrate (0.1 M in the case of water-soluble pentafluorophenol, pentafluorobenzoic acid, tetrafluorophthalic acid, and pentafluorosulfonic acid; 0.005 and 0.003 M for pentafluoropyridine and hexafluorobenzene, respectively), H_2O_2 (0.1, 0.8, or 2.6 M), and carbon-supported $(FePctBu_4)_2N$ catalyst [20 mg containing 0.2 μmol of $(FePctBu_4)_2N$]. The reactor was kept at 60 °C with magnetic stirring for 15 h. After the mixture was cooled to room temperature, the solid catalyst was separated by filtration and the reaction mixture was analyzed by GC−MS and ^{19}F NMR methods. The total organic carbon content was measured in several experiments.

■ ASSOCIATED CONTENT

Supporting Information

Experimental details, characterization data, and details of catalysis studies. This material is available free of charge via the Internet at http://pubs.acs.org.

■ AUTHOR INFORMATION

Corresponding Authors

alexander.sorokin@ircelyon.univ-lyon1.fr
pavel.afanasiev@ircelyon.univ-lyon1.fr

Notes

The authors declare no competing financial interest.

■ ACKNOWLEDGMENTS

Research support was provided by the Agence Nationale de Recherche (ANR, France, Grant ANR-08-BLANC-0183-01). C.C. is grateful to the Région Rhône-Alpes for Ph.D. fellowship. We thank Dr. D. Bouchu for the help with ESI-MS. We acknowledge the SOLEIL (Gif-sur-Yvette, France) and the ESRF (Grenoble, France) for provision of time on the SAMBA and ID26 beamlines, respectively. We thank Dr. V. Briois (SOLEIL), Dr. J. C. Swarbrick (ESRF), and Dr. M. Rovezzi (ESRF) for technical assistance.

■ REFERENCES

(1) Amii, H.; Uneyama, K. *Chem. Rev.* **2009**, *109*, 2119.
(2) Grushin, V. V. *Acc. Chem. Res.* **2010**, *43*, 160.

(3) (a) Douvris, C.; Ozerov, O. V. *Science* **2008**, *321*, 1188. (b) Perutz, R. N. *Science* **2008**, *321*, 1168.
(4) Clot, E.; Eisenstein, O.; Jasim, N.; Macgregor, S. A.; McGrady, J. E.; Perutz, R. N. *Acc. Chem. Res.* **2011**, *44*, 333.
(5) Baumgartner, R.; McNeill, K. *Environ. Sci. Technol.* **2012**, *46*, 10199.
(6) (a) Lv, H.; Cai, Y.-B.; Zhang, J.-L. *Angew. Chem., Int. Ed.* **2013**, *52*, 3203. (b) Yow, S.; Gates, S. J.; White, A. J. P.; Crimmin, M. R. *Angew. Chem., Int. Ed.* **2012**, *51*, 12559. (c) Reade, S. P.; Mahon, M. F.; Whittlesey, M. K. *J. Am. Chem. Soc.* **2009**, *131*, 1847. (d) Douvris, C.; Nagaraja, C. M.; Chen, C.-H.; Foxman, B. M.; Ozerov, O. V. *J. Am. Chem. Soc.* **2010**, *132*, 4946.
(7) Hackett, J. C.; Sanan, T. T.; Hadad, C. M. *Biochemistry* **2007**, *46*, 5924.
(8) (a) Sorokin, A.; Séris, J.-L.; Meunier, B. *Science* **1995**, *268*, 1163. (b) Sorokin, A.; Meunier, B. *Chem.—Eur. J.* **1996**, *2*, 1308. (c) Sorokin, A.; De Suzzoni-Dezard, S.; Poullain, D.; Noël, J.-P.; Meunier, B. *J. Am. Chem. Soc.* **1996**, *118*, 7410.
(9) Sorokin, A. B. *Chem. Rev.* **2013**, *113*, 8152.
(10) (a) Sorokin, A. B.; Kudrik, E. V.; Bouchu, D. *Chem. Commun.* **2008**, 2562. (b) Sorokin, A. B.; Kudrik, E. V.; Alvarez, L. X.; Afanasiev, P.; Millet, J.-M. M.; Bouchu, D. *Catal. Today* **2010**, *157*, 149. (c) Kudrik, E. V.; Sorokin, A. B. *Chem.—Eur. J.* **2008**, *14*, 7123. (d) İşçi, Ü.; Afanasiev, P.; Millet, J.-M. M.; Kudrik, E. V.; Ahsen, V.; Sorokin, A. B. *Dalton Trans.* **2009**, 7410. (e) Afanasiev, P.; Bouchu, D.; Kudrik, E. V.; Millet, J.-M. M.; Sorokin, A. B. *Dalton Trans.* **2009**, 9828. (f) Alvarez, L. X.; Kudrik, E. V.; Sorokin, A. B. *Chem.—Eur. J.* **2011**, *17*, 9298.
(11) Kudrik, E. V.; Afanasiev, P.; Alvarez, L. X.; Dubourdeaux, P.; Clémancey, M.; Latour, J.-M.; Blondin, G.; Bouchu, D.; Albrieux, F.; Nefedov, S. E.; Sorokin, A. B. *Nat. Chem.* **2012**, *4*, 1024.
(12) (a) Nyokong, T.; Gasyna, Z.; Stillman, M. J. *Inorg. Chem.* **1987**, *26*, 548. (b) Ough, E.; Gasyna, Z.; Stillman, M. J. *Inorg. Chem.* **1991**, *30*, 2301. (c) Afanasiev, P.; Kudrik, E. V.; Millet, J.-M. M.; Bouchu, D.; Sorokin, A. B. *Dalton Trans.* **2011**, *40*, 701.
(13) Glatzel, P.; Bergmann, U. *Coord. Chem. Rev.* **2005**, *249*, 65.
(14) (a) Chandrasekaran, P.; Stieber, S. C. E.; Collins, T. J.; Que, L., Jr.; Neese, F.; DeBeer, S. *Dalton Trans.* **2011**, *40*, 11070. (b) Jackson, T. A.; Rohde, J.-U.; Seo, M. S.; Sastri, C. V.; DeHont, R.; Stubna, A.; Ohta, T.; Kitagawa, T.; Münck, E.; Nam, W.; Que, L., Jr. *J. Am. Chem. Soc.* **2008**, *130*, 12394. (c) Aliaga-Alcalde, N.; Mienert, B.; Bill, E.; Wieghardt, K.; DeBeer George, S.; Neese, F. *Angew. Chem., Int. Ed.* **2005**, *44*, 2908. (d) Berry, J. F.; Bill, E.; Bothe, E.; DeBeer George, S.; Mienert, B.; Neese, F.; Wieghardt, K. *Science* **2006**, *312*, 1937. (e) de Oliveira, F. T.; Chanda, A.; Banerjee, D.; Shan, X.; Mondal, S.; Que, L., Jr.; Bominaar, E. L.; Münck, E.; Collins, T. J. *Science* **2007**, *315*, 835.
(15) Newcomb, M.; Halgrimson, J. A.; Horener, J. H.; Wasinger, E. C.; Chen, L. X.; Sligar, S. G. *Proc. Natl. Acad. Sci. U.S.A.* **2008**, *105*, 8179.
(16) (a) Delgado-Jaime, M. U.; Dible, B. R.; Chiang, K. P.; Brennessel, W. W.; Bergmann, U.; Holland, P. L.; DeBeer, S. *Inorg. Chem.* **2011**, *50*, 10709. (b) Pollock, C. J.; DeBeer, S. *J. Am. Chem. Soc.* **2011**, *133*, 5594.
(17) Lancaster, K. M.; Hu, Y.; Bergmann, U.; Ribbe, M. W.; DeBeer, S. *J. Am. Chem. Soc.* **2013**, *135*, 610.
(18) (a) Kadish, K. M.; Rhodes, R. K. *Inorg. Chem.* **1983**, *22*, 1090. (b) Kadish, K. M.; Bottomley, L. A. *Inorg. Chem.* **1981**, *20*, 1348.
(19) (a) Takahashi, A.; Yamaki, D.; Ikemura, K.; Kurahashi, T.; Ogura, T.; Hada, M.; Fujii, H. *Inorg. Chem.* **2012**, *51*, 7296. (b) Gross, Z. *J. Biol. Inorg. Chem.* **1996**, *1*, 368. (c) de Visser, S. P.; Tahsini, L.; Nam, W. *Chem.—Eur. J.* **2009**, *15*, 5577. (d) Kang, Y.; Chen, H.; Jeong, Y. J.; Lai, W.; Bae, E. H.; Shaik, S.; Nam, W. *Chem.—Eur. J.* **2009**, *15*, 10039.
(20) Bogachev, A. A.; Kobrina, L. S.; Yakobson, G. G. *Russ. J. Org. Chem.* **1986**, *22*, 2307.
(21) (a) Ravichandran, L.; Selvam, K.; Swaminathan, M. *J. Photochem. Photobiol., A* **2007**, *188*, 392. (b) Ravichandran, L.; Selvam, K.; Swaminathan, M. *Desalination* **2010**, *260*, 18.
(22) Bogachev, A. A.; Kobrina, L. S.; Yakobson, G. G. *Russ. J. Org. Chem.* **1986**, *22*, 2313.
(23) Osman, A. M.; Posthumus, M. A.; Veeger, C.; van Bladeren, P. J.; Laane, C.; Rietjens, I. M. C. M. *Chem. Res. Toxicol.* **1998**, *11*, 1319.
(24) Murphy, C. D. *Biotechnol. Lett.* **2009**, *32*, 351.
(25) Rietjens, I. M.; Vervoort, J. *Chem. Res. Toxicol.* **1992**, *5*, 10.
(26) (a) Kuehnel, M. F.; Lentz, D.; Braun, T. *Angew. Chem., Int. Ed.* **2013**, *52*, 3328. (b) Nova, A.; Mas-Ballesté, R.; Lledós, A. *Organometallics* **2012**, *31*, 1245. (c) Sun, L.; Rong, M.; Kong, D.; Bai, Z.; Yuan, Y.; Weng, Z. *J. Fluorine Chem.* **2013**, *150*, 117. (d) Arisawa, M.; Suzuki, T.; Ishikawa, T.; Yamaguchi, M. *J. Am. Chem. Soc.* **2008**, *130*, 12214.
(27) Liu, C.; Cao, L.; Yin, X.; Xu, H.; Zhang, B. *J. Fluorine Chem.* **2013**, *156*, 51.
(28) An NIH shift is the migration of a substituent at a hydroxylation site to an adjacent position. See: (a) Jerina, D. M.; Daly, J. W. *Science* **1974**, *185*, 573. (b) de Visser, S. P.; Shaik, S. *J. Am. Chem. Soc.* **2003**, *125*, 7413. (c) Mitchell, K. H.; Rogge, C. E.; Gierahn, T.; Fox, B. G. *Proc. Natl. Acad. Sci. U.S.A.* **2003**, *100*, 3784.
(29) Rietjens, I. M.; den Besten, C.; Hanzlik, R. P.; van Bladeren, P. J. *Chem. Res. Toxicol.* **1997**, *10*, 629.
(30) Koerts, J.; Soffers, A. E.; Vervoort, J.; De Jager, A.; Rietjens, I. M. *Chem. Res. Toxicol.* **1998**, *11*, 503.
(31) (a) Daly, J. W.; Jerina, D. M.; Witkop, B. *Experientia* **1972**, *28*, 1129. (b) Schwartz, H.; Chu, I.; Villeneuve, D. C.; Benoit, F. M. *J. Toxicol. Environ. Health* **1987**, *22*, 341. (c) Bogaards, J. J. P.; Van Ommen, B.; Wolf, C. R.; Van Bladeren, P. J. *Toxicol. Appl. Pharmacol.* **1995**, *132*, 44.
(32) Rietjens, I. M. C. M.; Vervoort, J. *Xenobiotica* **1989**, *19*, 1297.
(33) Sisemore, M. F.; Selke, M.; Burstyn, J. N.; Valentine, J. S. *Inorg. Chem.* **1997**, *36*, 979.
(34) (a) Adams, D. E. C.; Halden, R. U. *ACS Symp. Ser.* **2010**, *1048*, 539−560. (b) Murphy, M. B.; Loi, E. I. H.; Kwork, K. Y.; Lam, P. K. S. In *Fluorous Chemistry*; Horvath, I., Ed.; Springer: Berlin, 2011; pp 339−364.
(35) Shteingarts, V. D. *J. Fluorine Chem.* **2007**, *128*, 797 and references therein.
(36) Ankudinov, A. L.; Bouldin, C. E.; Rehr, J. J.; Sims, J.; Hung, H. *Phys. Rev. B* **2002**, *65*, 104.
(37) Klementiev, K. V. *J. Synchrotron Radiat.* **2001**, *8*, 270.
(38) Bellack, E.; Schouboe, P. J. *Anal. Chem.* **1958**, *30*, 2032.
(39) Metz, J.; Schneider, O.; Hanack, M. *Inorg. Chem.* **1984**, *23*, 1065.